A two-dimensional NMR study of the solution structure of a DNA dodecamer comprising the concensus sequence for the specific DNA-binding sites of the glucocorticoid receptor protein

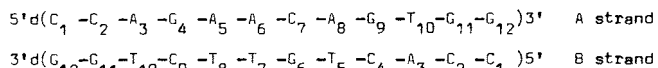G. Marius CLORE, Hanspeter LAUBLE, Thomas A. FRENKIEL, and Angela M. GRONENBORN

Division of Physical Biochemistry and Medical Research Council Biomedical Nuclear Magnetic Resonance Centre, National Institute for Medical Research, London

A two-dimensional 500-MHz ^{1}H-NMR study on the non-self-complementary double-stranded DNA dodecamer 5′d(C-C-A-G-A-A-C-A-G-T-G-G)5′d(C-C-A-C-T-G-T-T-C-T-G-G), is presented. This oligonucleo-tide contains the consensus octanucleotide sequence 5′d(A-G-A-A-C-A-G-T) for the specific DNA-binding sites of the glucocorticoid receptor protein [Payvar, F. et al. (1984) *Cell 35*, 381 – 392]. Using a combination of two-dimensional pure phase absorption nuclear Overhauser enhancement (NOESY) and homonuclear *J*-correlated (COSY) spectroscopy all non-exchangeable base (with the exception of the adenine H2 protons), methyl and deoxyribose H1′, H2′, H2″, H3′ and H4′ resonances are assigned unambiguously using a sequential resonance assignment strategy. From the relative intensities of the cross peaks in the pure phase absorption NOESY spectra at two mixing times it is shown that the dodecamer adopts a B-type conformation in solution.

The glucocorticoid receptor protein stimulates transcription of integrated proviral mammary tumour virus genes in a variety of cell lines derived from mouse mammary tumours [1, 2]. Recent mapping and nuclease footprinting experiments have demonstrated the presence of five regions of mammary tumour virus DNA that are bound specifically by the purified glucocorticoid receptor protein [3, 4]. One of these regions resides upstream of the transcription start site, and the others are located within transcribed sequences 4000 – 8000 bases from the initiation site [3]. Within each region there are a number of DNA sequences varying in length between 15 and 44 base pairs which are protected in the footprinting experiments [3, 4]. These sequences are characterized by the degenerate 8-base-pair consensus sequence 5′d(A-G-A-A/T-C-A-G-A/T) [3].

As an initial step in the study of the structural and dynamic aspects of specific DNA-glucocorticoid receptor protein interactions, we have carried out a two-dimensional NMR study of the solution structure of the non-self-complementary DNA dodecamer

$$5'd(C_1 - C_2 - A_3 - G_4 - A_5 - A_6 - C_7 - A_8 - G_9 - T_{10} - G_{11} - G_{12})3' \quad \text{A strand}$$

$$3'd(G_{12} - G_{11} - T_{10} - C_9 - T_8 - T_7 - G_6 - T_5 - C_4 - A_3 - C_2 - C_1)5' \quad \text{B strand}$$

which contains the above octanucleotide consensus sequence. The mainstay of the present study lies in the use of the nuclear Overhauser enhancement (NOE) to demonstrate the proximity of protons in space [5 – 8]. In particular, we have made use of the two-dimensional method of detecting NOEs [9 – 11], an experiment known as NOESY (two-dimensional nuclear Overhauser enhancement spectroscopy). In addition, we have employed two-dimensional homonuclear *J*-correlated spectroscopy (COSY) to identify spins belonging to the same homonuclear scalar coupling network [12, 13]. By making use of the information obtained from the NOESY and COSY

Abbreviations. NOE, nuclear Overhauser enhancement; NOESY, two-dimensional nuclear Overhauser enhancement spectroscopy; COSY, two-dimensional homonuclear *J*-correlated spectroscopy.

spectra, all non-exchangeable base (with the exception of the adenine H2 protons), methyl and deoxyribose H1′, H2′, H2″, H3′ and H4′ proton resonances are assigned sequentially in a similar manner to that pioneered for protein spectra by Wüthrich and his collaborators [14 – 16]. Moreover, information about the build-up rates of the NOEs can be deduced by acquiring pure phase absorption NOESY spectra with different mixing times [17]; and it is shown from the relative magnitudes of the cross peaks in two such spectra that the dodecamer adopts a B-type conformation in solution.

EXPERIMENTAL PROCEDURE

The two strands of the dodecamer, 5′d(C-C-A-G-A-A-C-A-G-T-G-G) and 5′(C-C-A-C-T-G-T-T-C-T-G-G), were prepared from suitably protected nucleosides according to the phosphitetriester method [18] principally as described by Seliger et al. [19] and purified by reverse-phase high-pressure liquid chromatography using a Waters μBondapak C_{18} column. After desalting and extensive lyophilisation, the two strands of the dodecamer (final concentration 8 mM per strand) were taken up in 99.96% D_2O containing 100 mM KCl, 10 mM potassium phosphate pH* 6.8 (meter reading uncorrected for the isotope effect on the glass electrode) and 0.02 mM EDTA, and annealed by heating to 80 C and subsequent slow cooling.

The temperature used for all NMR experiments was 25 C. Under these conditions of ionic strength and temperature, the two strands of the dodecamer are entirely in the duplex state as judged from terminal denaturation studies (unpublished data).

All NMR spectra were recorded on a Bruker AM 500 spectrometer equipped with an Aspect 3000 computer. Quadrature detection was used with the carrier placed at the position of the residual HOD resonance, approximately in the middle of the nucleic acid spectrum.

COSY spectra were recorded with a squence of two non-selective 90 pulses [12, 13]: 90 -t_1-90 -t_2-d. The phases of the

pulses and of the receiver were cycled to provide quadrature information in the F1 dimension and to eliminate axial peaks [20]. The delay t_1 is the evolution period characteristic of two-dimensional NMR. 256 t_1 values were used with a step size of 266 μs and an initial value of zero; 128 transients were acquired for each increment. Data was sampled during the detection period t_2 (0.272 s), whilst the delay d (0.8 s) was inserted to allow the spin system to recover between transients. The same spectral width (3760 Hz) was used in each dimension. Prior to Fourier transformation the time-domain data were multiplied by a sine-squared bell shifted by π/128 and π/64 in the t_2 and t_1 directions respectively, corresponding to a considerable degree of resolution enhancement. Zero-filling was employed in the t_1 dimension to result in a frequency-domain matrix of size 1 K × 1 K, with digital resolution equal to 3.67 Hz per point in each dimension. The spectrum is presented in the absolute-value mode and has been improved by symmetrization [21].

The basic NOESY experiment [9] consists of a sequence of three 90 pulses: 90 -t_1-90 -τ_m-90 -t_2-d; exchange of longitudinal magnetization occurs during the mixing time τ_m. Two modifications of the original experiment have recently been described [22, 23]: both give peaks with pure double-absorption line shapes whilst retaining the advantages that result from the use of quadrature detection in the F1 dimension. This work made use of one of these methods, that of Marion and Wüthrich [23], and the phase cycling and data processing were done according to their procedure. The phase cycling also provided for the suppression of axial peaks and of cross peaks due to coherence transfer via multiple-quantum coherence [24], though no special method was used to prevent cross peaks arising from zero-quantum coherence transfer. The detection period t_2 and relaxation delay d have the same functions as in the COSY spectrum and were set to values of 0.265 s and 0.8 s respectively. A spectral width equal to 4000 Hz was obtained in the F1 dimension by incrementing the evolution period t_1 in steps of 125 μs; 128 transient were collected for each of 700 increments, and a spectral width of 4000 Hz was also used in the F2 dimension. A square 1 K × 1 K frequency-domain data matrix was obtained by zero-filling in t_1, giving a digital resolution of 3.91 Hz per point in each dimension. Apodization and mild resolution enhancement were applied by multiplying the time-domain data with a sine-squared bell, shifted by π/4 in both the t_1 and t_2 dimensions. An initial phase correction was carried out during the transformation with a final adjustment after completion of the two-dimensional transform. These manipulations were followed by symmetrization [21].

Pure phase absorption NOESY spectra were obtained with two different mixing times, namely 100 ms and 300 ms, both of which are short enough to avoid excessive spin diffusion [17, 25].

All two-dimensional spectra are presented as contour plots with successive contour levels incremented on a linear scale. Chemical shifts are expressed relative to 4,4-dimethylsilapentane-1-sulfonate.

RESULTS AND DISCUSSION

First level resonance assignment

The assignment of resonance type is easily achieved by comparison with the spectra of nucleotides and other small oligonucleotides [26, 27]. In this manner various spectral regions can be defined: the base H8, H6 and H2 resonances lie between 7 ppm and 8.5 ppm, the H1' sugar and cytosine H5 resonances between 5 ppm and 6.3 ppm, the H3' sugar resonances between 3.5 ppm and 4.5 ppm, the H2' and H2'' sugar resonances between 1.8 ppm and 3 ppm, and the methyl proton resonances of the thymine residues between 1 ppm and 1.8 ppm.

To complete the first level resonance assignment it is helpful to identify spin systems by means of a COSY spectrum. In this manner the J connectivities between the H5 and H6 resonances of the cytosine residues (see Fig. 2 below), and between the H6 and methyl resonances of the thymine residues (via their four-bond spin-spin coupling; see Fig. 3 below) are easily established. In addition the sugar resonances could in principle be grouped into families of signals belonging to the same network of coupled spins via the intranucleotide pathway H1'↔H2'/H2''↔H3'↔H4'↔H5'/H5''. In practice, however, this is usually restricted to the H1'↔H2'/H2'' connectivities as the chemical shift dispersion of the H3', H4', H5' and H5'' resonances is too limited.

Sequential assignment of individual resonances

In order to assign individual resonances we have made use of pure phase absorption two-dimensional nuclear Overhauser enhancement (NOE) measurements [9, 22, 23]. In an analogous manner to one-dimensional NOE measurements [28, 29] the intensity of a cross peak between resonances i and j, a_{ij}, at short values of the mixing time τ_m in a NOESY spectrum is given by [10, 17]

$$a_{ij} \approx \sigma_{ij}\tau_m$$

where σ_{ij} is the cross-relaxation rate between protons i and j. σ_{ij} is in turn proportional to r_{ij}^{-6} where r_{ij} is the distance between protons i and j [30]. As a result, the intensity of a cross peak is very sensitive to interproton distance, decreasing rapidly as r_{ij} increases and becoming virtually undetectable for $r_{ij} \gtrsim 0.5$ nm.

Bearing in mind the above properties of the NOE, sequential resonance assignment strategies, based on the known structures of right-handed DNA have been put forward independently by a number of groups [31−43]. A comprehensive strategy for the assignment of the H8, H6 and H5 base protons, the methyl protons and the sugar protons in right handed DNA helices is summarized in Fig. 1. This scheme does not include the adenine H2 protons which together with the exchangeable imino and amino protons are part of a separate cross-relaxation network [8, 33, 34, 44−48].

It is particularly important to note that the application of the scheme shown in Fig. 1 for the NOE-based sequential resonance assignment strategy does not require the initial assumption of a right-handed helical structure for the following reasons. First, the general pattern of NOEs observed for right-handed A and B type helices is quite different from that expected for left-handed Z DNA, and this is easily ascertained from simple inspection of the complete NOESY spectrum. Second, the additional demands, constraints and information extracted from the J connectivities, the known nucleotide sequence, the nature of the terminal residues, and, most of all, the directionality of some of the internucleotide NOEs, makes the assignments based on the NOE data completely unambiguous. Furthermore, independent evidence as to the helical state of a particular oligonucleotide can always be obtained from a circular dichroic spectrum, which in this case is indicative of a right-handed B-type conformation (unpublished data).
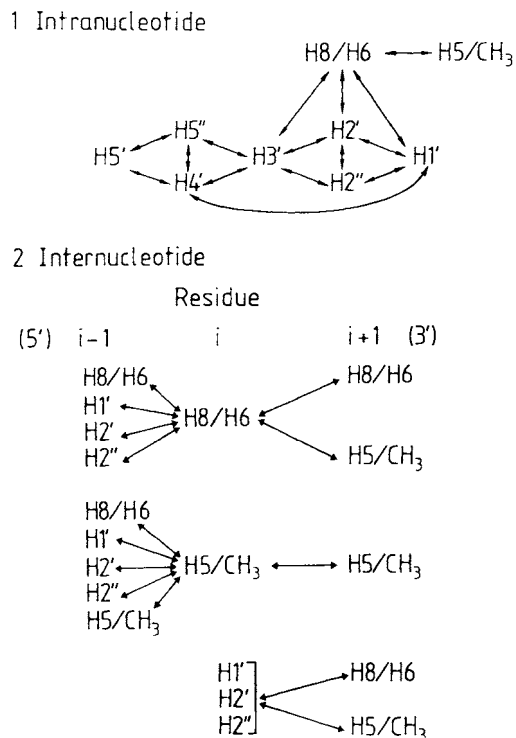
1 Intranucleotide

H8/H6 ⟷ H5/CH₃

2 Internucleotide

Residue

(5') i-1   i   i+1 (3')

The various pertinent regions of the NOESY spectra used for the sequential resonance assignment are shown in Fig. 2–6. The mainstay of the sequential assignment lies in the NOEs between the H8/H6 base protons and H1′ (Fig. 2) and H2′/H2″ (Fig. 3) sugar protons. This is because each H8/H6 base proton exhibits an NOE with H1′, H2′ and H2″ sugar protons of its own residue (i) and of the adjacent 5′-residue (i-1). In this manner, the H8/H6, H1′, H2′ and H2″ protons of both strands can be assigned sequentially. This procedure is aided by the observation of a number of additional intranucleotide NOEs and of several internucleotide NOEs between each pair of residues. The relevant intranucleotide NOEs are those between the C(H5) and C(H6) protons (Fig. 2), between the T(H6) and T(CH₃) protons (Fig. 3) and between the H1′ and H2′/H2″ protons (Fig. 4). (Note that these connectivities are also observed in the COSY spectrum as they involve resolvable scalar couplings.) Particularly helpful internucleotide NOEs are those between the C(H5) and adjacent 5′ H8/H6 protons (Fig. 2), between the T(CH₃) and adjacent 5′ H8/H6 (Fig. 3) and H1′ (Fig. 4) protons, between neighbouring C(H5) and T(CH₃) protons (Fig. 3), and between neighbouring H8/H6 protons (Fig. 5).

As an example, let us consider the B chain. We note that the sequence d(G₆ᵦ-T₇ᵦ-T₈ᵦ) is unique in the duplex dodecamer. Examination of the NOESY spectrum in Fig. 3 B immediately establishes the assignment of the methyl and base protons of these three residues via the NOE pathway G₆ᵦ(H8)↔T₇ᵦ(CH₃)↔T₇ᵦ(H6)↔T₈ᵦ(CH₃)↔T₈ᵦ(H6). With this knowledge in mind, one need only turn to the NEOSY spectrum in Fig. 2 and 3A to establish NOE connectivities between the H8/H6 and H1′ protons and between the H8/H6 and
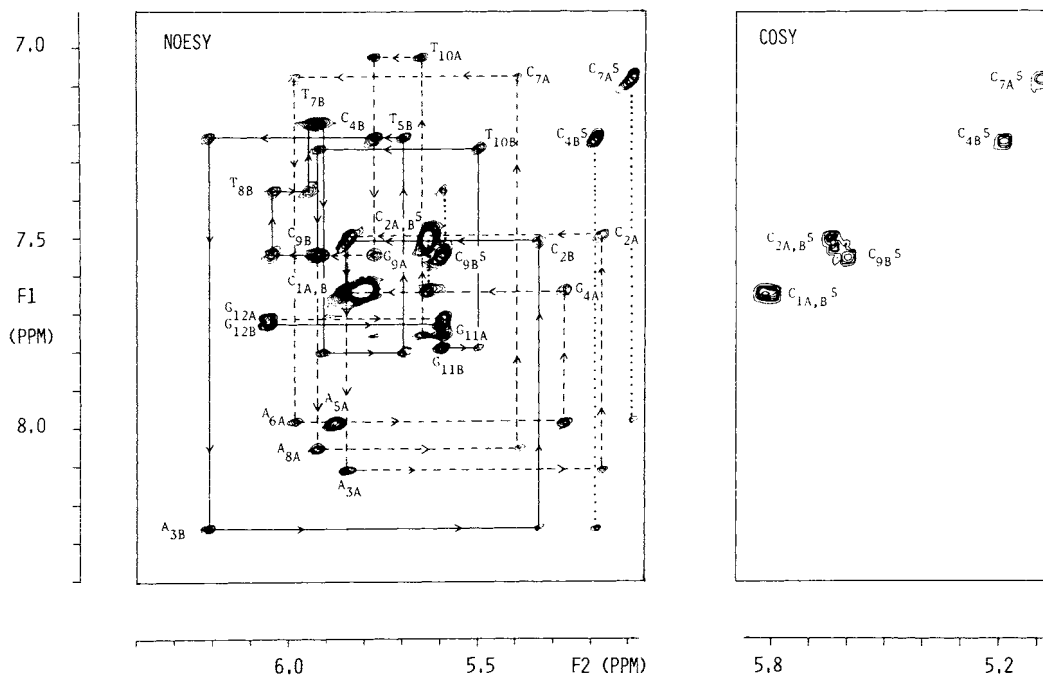
Fig. 1. *Schematic illustration of the intranucleotide and internucleotide distances with values of ≲ 0.5 nm in right-handed DNA which form the basis of the sequential resonance assignment procedure by means of NOE measurements.* These distance relationships are applicable to both B and A DNA [31, 33, 36, 49]

Fig. 2. *H8/H6(F1 axis) – H1′/H5(F2 axis) region of the pure phase absorption NOESY (300-ms mixing time) and absolute value COSY spectra.* The H1′(i–1)↔H8/H6(i)↔H1′(i) NOE connectivities are represented by interrupted (— — —) and continuous (———) lines for the A and B strands of the dodecamer respectively. H8/H6(i–1)–H5(i) NOE connectivities are indicated by the dotted lines (· · · ·). The H1′ and C(H5) protons are indicated as Nᵢ and Cᵢ5 respectively in the figure
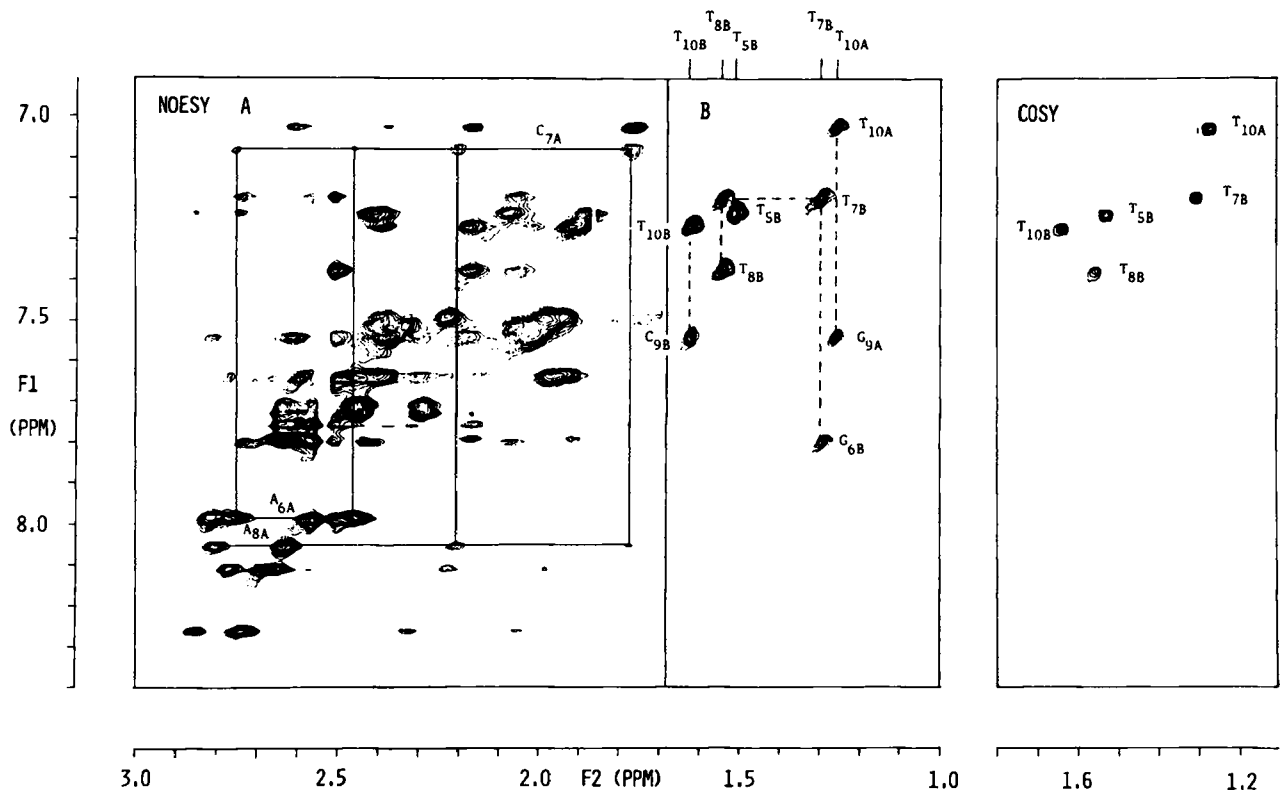
Fig. 3. (A) H8/H6 (F1 axis) — H2'/H2" (F2 axis) and (B) H8/H6(F1 axis) — CH₃ (F2 axis) regions of the pure phase absorption NOESY spectrum (mixing time of 300 ms). An absolute value COSY spectrum of the H8/H6(F1) — CH₃(F2) region is also shown. An example of the H2' H2" (i − 1)↔H8/H6 (i)↔H2'/H2" (i) NOE connectivities is indicated by the continuous line (——) for the A₆ₐ-C₇ₐ-A₈ₐ sequence of the A chain. The interrupted lines (-----) in (B) indicate H8/H6(i − 1)—CH₃(i) NOE connectivities. The assignments by the side of the cross peaks in B refer to the F1 axis
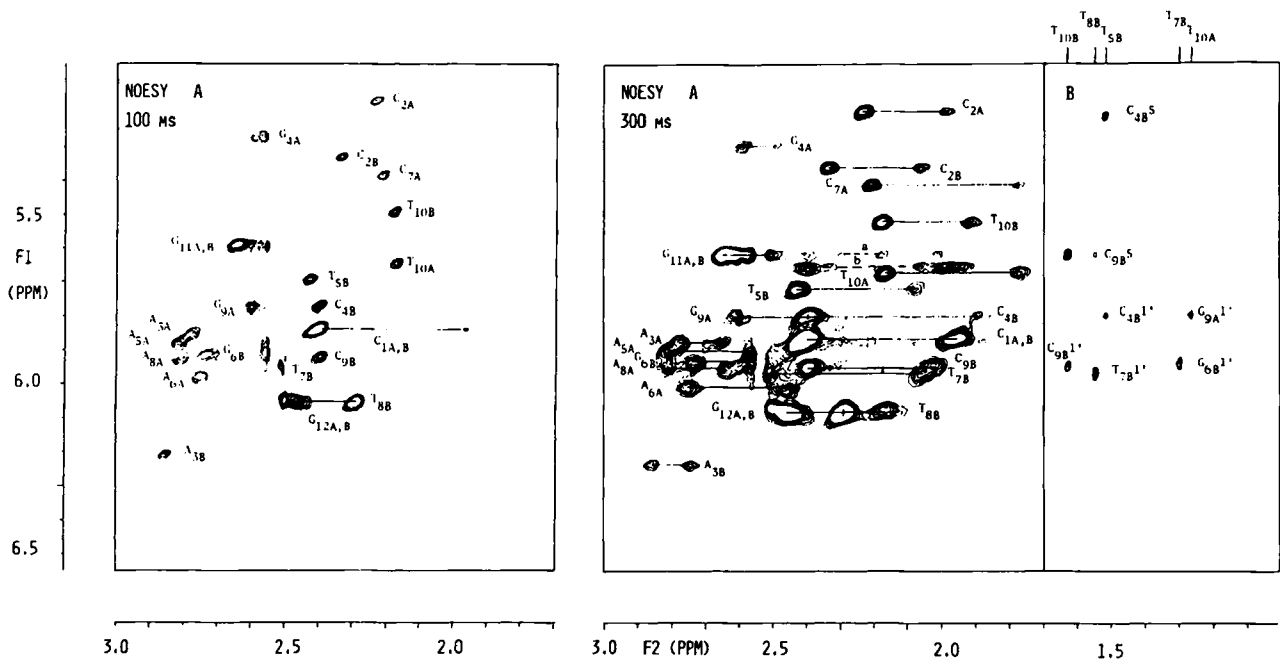

Fig. 4. (A) H1' H5 (F1 axis) — H2'/H2" (F2 axis) and (B) H1'/H5 (F1 axis) — CH₃ (F2 axis) regions of the pure phase absorption NEOSY spectra. The H1' H5(F1 axis) — H2'/H2"(F2 axis) region is shown for two mixing times (100 ms and 300 ms) with identical contour levels. Note that in the spectrum with the 100-ms mixing time the only H1'—H2' cross peaks that can be seen are those involving residues C₁ₐ and C₁ᴮ. and G₁₂ₐ and G₁₂ᴮ. The assignments by the side of the cross peaks in B refer to the F1 axis
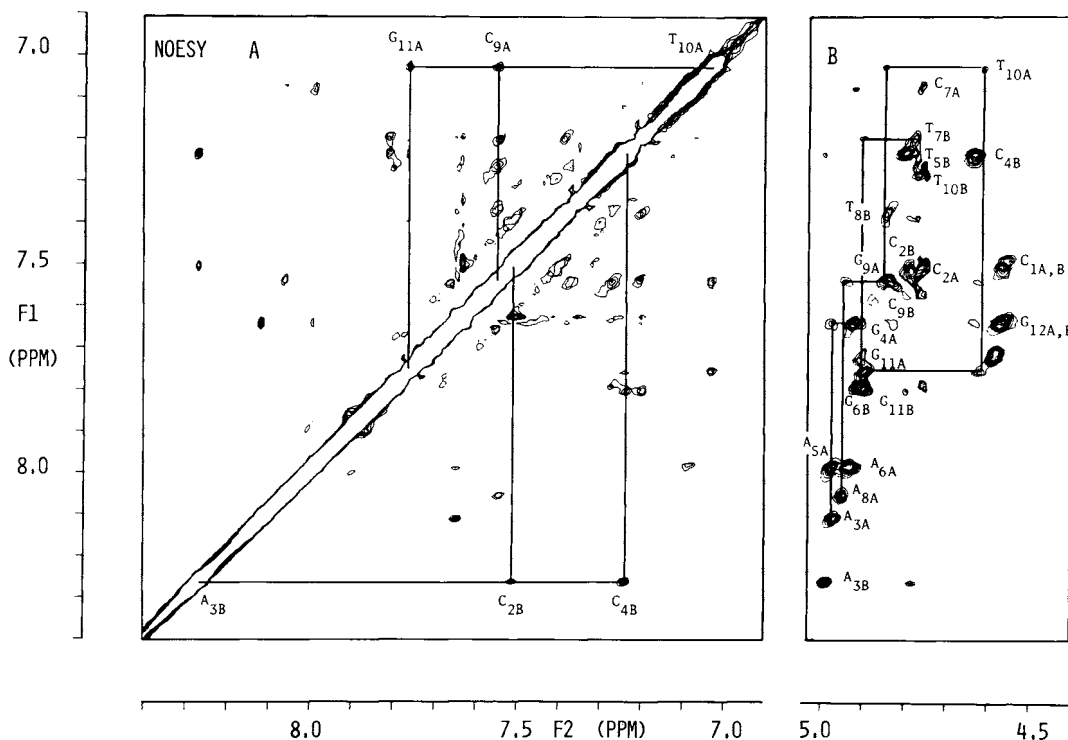
Fig. 5. *(A) H8/H6 (F1 axis) — H8/H6 (F2 axis) and (B) H8/H6 (F1 axis) — H3' (F2 axis) regions of the pure phase absorption NOESY spectrum (mixing time 300 ms).* In (A) two examples of internucleotide NOEs between adjacent H8/H6 protons are indicated. In (B) a few examples of $H3'(i-1) \leftrightarrow H8/H6(i) \leftrightarrow H3'(i)$ connectivities are also indicated [note that the internucleotide step occurs principally through the indirect $H3'(i-1) \leftrightarrow H2'/H2''(i-1) \leftrightarrow H8/H6(i)$ pathway]. The assignments by the side of the cross peaks in A refer to the F2 axis
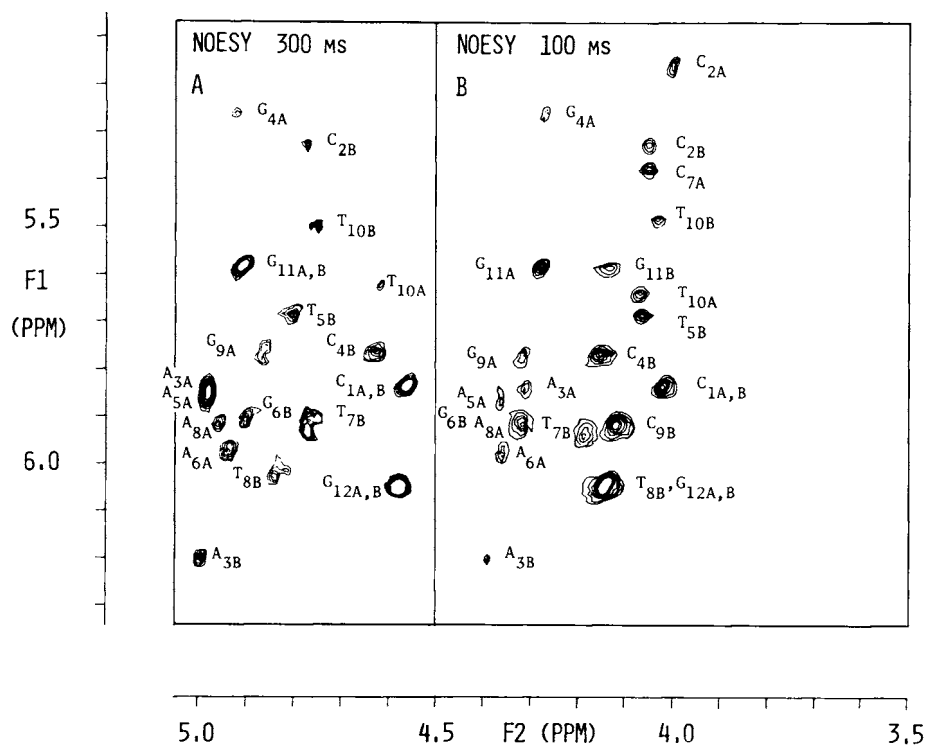

Fig. 6. *(A) H1' (F1 axis) — H3' (F2 axis) and (B) H1' (F1 axis) — H4' (F2 axis) regions of the pure phase absorption NOESY spectrum with mixing times of 300 and 100 ms respectively*

H2'/H2″ protons, respectively, of these residues, thereby providing a useful starting point with which to extend the assignment of the B-chain H8/H6, H1′ and H2′/H2″ protons in both directions.

With the base, methyl, H1′ and H2′/H2″ protons assigned, all that is required is to assign the H3′ and H4′ protons via the relevant intranucleotide connectivities. Thus intranucleotide NOEs are observed between the H3′ protons and the H8/H6 (Fig. 5B) and H1′ (Fig. 6A) protons. The latter arise principally through the indirect H1′↔H2′/H2″↔H3′ pathway. In addition to intranucleotide NOEs, internucleotide NOEs are also observed in the H8/H6−H3′ region of the NOESY spectrum (Fig. 5B). These occur between the H8/H6 and adjacent 5′H3′ protons primarily through the indirect H3′(i)↔H2′/H2″(i)↔H8/H6(i + 1) pathway. The H4′ protons are readily assigned from the intranucleotide NOEs between the H1′ and H4′ protons (Fig. 6B) and any ambiguities can readily be resolved from the observation of cross peaks in the NOESY spectrum at long mixing times arising from indirect intranucleotide NOEs between the H8/H6 and H4′ protons (data not shown).

All that is left to complete the assignments is to distinguish the H2′ from the H2″ protons. This is easily achieved by two independent methods. First, the intranucleotide separation between the H8/H6 and H2′ protons is always smaller than that between the H8/H6 and H2″ protons for all glycosidic bond torsion angles within the *anti* range characteristic of right-handed DNA conformations. Hence the intensity of the cross peaks arising from intranucleotide NOEs between the H8/H6 and H2′ protons will always be larger than that arising from the corresponding intranucleotide H8/H6−H2″ NOEs. This is apparent from the contour plot of the H8/H6−H2′/H2″ region of the NOESY spectrum with a 300-ms mixing time (Fig. 3A). This can also be appreciated from cross-sections as illustrated in Fig. 7A which shows a cross-section with the T_{10A}(H6) resonance at the position of the diagonal obtained from NOESY spectra with mixing times of 100 ms and 300 ms. The smaller intensity of the intranucleotide NOE between the T_{10A}(H6) and T_{10A}(H2″) protons relative to that between the T_{10A}(H6) and T_{10A}(H2′) protons is clear in the cross-section taken with the 100-ms mixing time; at 300 ms, however, the difference is reduced owing to spin diffusion. The second approach involves the observation that for all deoxyribose pucker conformations the distance between the H1′ and H2″ protons is usually shorter and can never be longer than that between the H1′ and H2′ protons. This is clearly manifested in the contour plots of the H1′−H2′/H2″ region of the NOESY spectra obtained with mixing times of 100 ms and 300 ms (Fig. 4A). A more accurate representation of the relative intensities of the H1′−H2′ and H1′−H2″ cross peaks is afforded by cross-sections as illustrated for the cross-section with C_{2B}(H1′) resonance at the position of the diagonal (Fig. 7B).

Unfortunately the assignment of the H5′ and H5″ protons for this particular oligonucleotide presents an intractable problem as the relevant cross peaks in both the NOESY and COSY spectra occur within regions of severe overlap and limited spectral dispersion. In this particular case the only assignments of H5′ and H5″ resonances that could be accomplished unambiguously were those of the C_{1A}, C_{1B} and A_{3B} residues. In the case of the C_{1A} and C_{1B} residues the resonances of the H5′ and H5″ protons are superimposed at 3.67 ppm, lying just to high field of the main bulk of the H4′, H5′ and H5″ resonances; in the case of the A_{3B} residue, the A_{3B}(H4′) resonance is the lowest field resonance in the H4′/
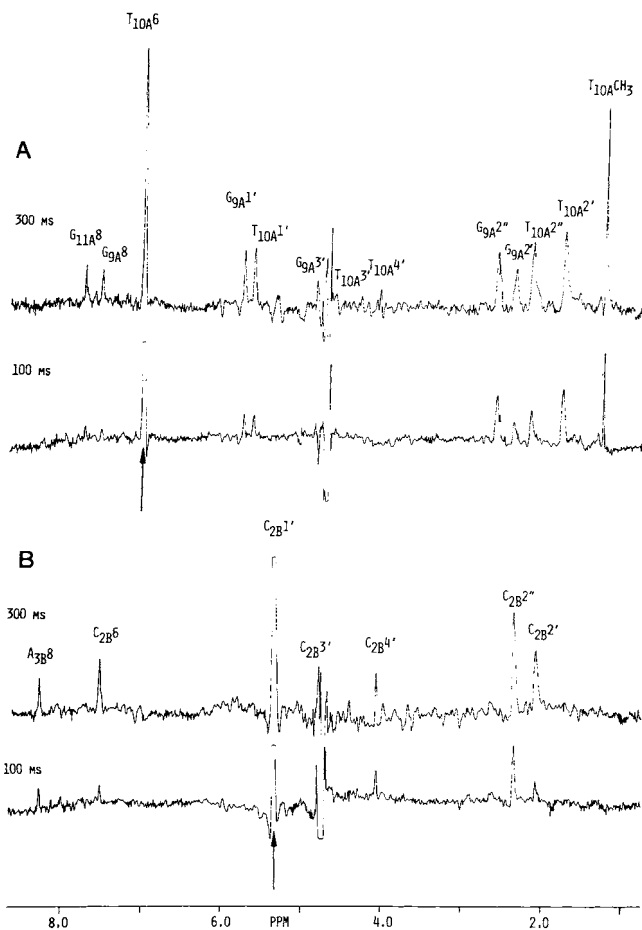

Fig. 7. *Cross-section of the pure phase absorption NOESY spectra (100-ms and 300-ms mixing times) taken with (A) the T_{10A}(H6) resonance and (B) the C_{2B}(H1′) resonance at the position of the diagonal.* These cross-sections correspond to the NOE difference spectra that would be observed in conventional one-dimensional spectroscopy upon selective inversion of the T_{10A}(H6) and C_{2B}(H1′) resonances

H5′/H5″ region thereby allowing the pairwise assignment of the A_{3B}(H5′) and A_{3B}(H5″) resonances at 3.91 ppm and 4.11 ppm from cross peaks in both the NOESY and COSY spectra.

The assignments of the H8, H6 and H5 base protons, the methyl protons and the H1′, H2′, H2″, H3′ and H4′ sugar protons in Table 1. A summary of all the observed internucleotide NOEs is shown in Fig. 8.

Low-resolution structure of the duplex dodecamer

Because at short mixing times the cross-peak intensities in the pure phase absorption NOESY spectra are approximately proportional to r^{-6}, the relative magnitudes of the various cross peaks provide a sensitive probe of molecular structure and enable one to define a low-resolution solution structure on the basis of a qualitative interpretation alone. A word of caution, however, should be added in interpreting relative cross-peak intensities in a simple manner as slight distortions may be introduced as a result of spin diffusion (even at the short mixing time employed here), data manipulation (viz. symmetrization and mild resolution enhancement), contributions from non-dipolar relaxation, in particular zero quantum coherence transfer between coupled spins, and

Table 1. *Assignments of the non-exchangeable proton resonances of the duplex dodecamer*
Chemical shifts (from 4,4-dimethylpentane-1-sulphonate) are at 25°C

| Residue	Chemical shift of protons						
	H8/H6	H5/CH$_3$	H1'	H2'	H2"	H3'	H4'
A strand	ppm						
C$_{1A}$	7.65	5.79	5.84	1.95	2.39	4.56	4.01
C$_{2A}$	7.52	5.62	5.16	1.97	2.22	4.76	3.99
A$_{3A}$	8.13		5.84	2.65	2.79	4.97	4.29
G$_{4A}$	7.66		5.26	2.47	2.58	4.91	4.25
A$_{5A}$	8.00		5.86	2.56	2.80	4.97	4.34
A$_{6A}$	8.00		5.97	2.45	2.74	4.93	4.34
C$_{7A}$	7.05	5.07	5.37	1.76	2.20	4.76	4.04
A$_{8A}$	8.07		5.92	2.64	2.80	4.94	4.31
G$_{9A}$	7.56		5.75	2.38	2.60	4.83	4.30
T$_{10A}$	7.04	1.26	5.64	1.76	2.16	4.62	4.07
G$_{11A}$	7.77		5.58	2.50	2.63	4.89	4.27
G$_{12A}$	7.73		6.04	2.45	2.29	4.57	4.13
B strand							
C$_{1B}$	7.65	5.79	5.84	1.95	2.39	4.56	4.01
C$_{2B}$	7.52	5.62	5.32	2.05	2.32	4.79	4.04
A$_{3B}$	8.23		6.20	2.73	2.86	4.98	4.30
C$_{4B}$	7.25	5.18	5.76	1.89	2.38	4.63	4.14
T$_{5B}$	7.25	1.51	5.68	2.08	2.42	4.80	4.06
G$_{6B}$	7.81		5.90	2.55	2.72	4.91	4.31
T$_{7B}$	7.21	1.29	5.93	2.06	2.51	4.79	4.19
T$_{8B}$	7.39	1.54	6.03	2.15	2.29	4.83	4.13
C$_{9B}$	7.55	5.58	5.91	2.03	2.38	4.81	4.11
T$_{10B}$	7.28	1.61	5.48	1.90	2.17	4.72	4.03
G$_{11B}$	7.80		5.58	2.50	2.63	4.91	4.13
G$_{12B}$	7.75		6.04	2.44	2.29	4.57	4.13
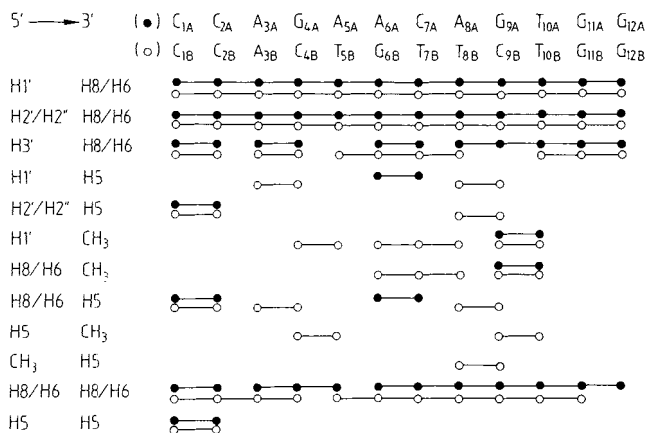
Fig. 8. *Summary of the internucleotide NOEs observed for the A (●) and B (○) strands of the dodecamer*

variations in effective correlation time for different interproton vectors. These problems and their resolution for quantitative analysis of pre-steady-state NOE data on oligonucleotides have been discussed by ourselves in detail elsewhere [35, 54]. Nevertheless, the qualitative approach used here is adequate for distinguishing between A, B and Z DNA.

Considering the intranucleotide NOEs first we note the following pattern of cross-peak intensities: $a_{H2'-H8/H6} \gg a_{H1'-H8/H6} > a_{H3'-H8/H6}$ for the sugar-base NOEs and $a_{H2''-H1'} > a_{H2'-H1'} > a_{H1'-H4'}$ for the intrasugar NOEs. This

pattern of NOEs is indicative of an *anti* conformation about the glycosidic bond within the range $\chi \approx -115 \pm 30°$ and a deoxyribose conformation in the C1'-*exo* to C2'-*endo* range [33–35] characteristic of B DNA [49–51]. In the case of A DNA which has a low *anti* glycosidic bond conformation ($\chi \approx -160 \pm 10°$) and C3'-*endo* sugar pucker [49, 52, 53] the pattern of cross-peak intensities observed for the sugar-base NOEs would be $a_{H3'-H8/H6} \gg a_{H1'-H8/H6} \approx a_{H2'-H8/H6}$.

The overall solution structure of the dodecamer can be ascertained from the internucleotide NOEs (see Fig. 8). With the exception of the internucleotide NOEs between adjacent H8/H6 protons and between adjacent H5/CH$_3$ protons, all the internucleotide NOEs exhibit directional specificity. Thus, for example, internucleotide NOEs are observed between the H1', H2' and H2" sugar protons of the ith residue and the H8/H6 base proton of the ($i + 1$) residue but not the ($i - 1$) residue, and similarly between the T(CH$_3$) protons of the ith residue and the H8/H6 proton of the ($i - 1$) residue but not the ($i + 1$) residue. This pattern of NOEs is only compatible with an overall right-handed helical structure [31–35, 55]. The distinction between the A and B-type geometries can be made on the basis of the relative magnitudes of the intranucleotide and internucleotide NOEs between the H8/H6 and H2'/H2" protons. In the present case, the pattern of cross-peak intensities is as follows: $a_{H2'(i)-H8/H6(i)} \gg a_{H2''(i-1)-H8/H6(i)} > a_{H2'(i-1)-H8/H6(i)}$, confirming the overall B type structure [31–35]. In A DNA the observed pattern would be $a_{H2'(i-1)-H8/H6(i)} \gg a_{H2''(i-1)-H8/H6(i)} > a_{H2'(i)-H8/H6(i)}$.

CONCLUDING REMARKS

In the present paper we have demonstrated the power of pure phase absorption NOESY spectroscopy in obtaining reliable resonance assignments and low-resolution structural information on a relatively long non-self-complementary double-stranded oligonucleotide, namely a duplex dodecamer comprising the octanucleotide consensus sequence for the specific DNA binding sites of the glucocorticoid receptor protein. This data provides the essential basis not only for examining the specific DNA-glucocorticoid receptor protein interaction but also for obtaining a high-resolution structure for the dodecamer in solution. The latter involves determining accurate interproton distances from the initial build up rates of the NOEs followed, for example, by a constrained least-squares minimization in which all covalent bond lengths, fixed bond angles, van der Waal's contacts, and hydrogen bond lengths and geometry are constrained within narrow limits in order to refine an initial trial model on the basis of the experimentally determined interproton distances.

REFERENCES

1. Ringold, G. M., Yamamoto, K. R., Bischop, J. M. & Varmus, H. E. (1977) *Proc. Natl Acad. Sci. USA 74*, 2879–2883.
2. Ucker, D. S., Ross, S. R. & Yamamoto, K. R. (1981) *Cell 27*, 257–266.

636

3. Payvar, F., De Franco, D., Firestone, G. L., Edgar, B., Wrange, O., Okret, S., Gustafson, J. A. & Yamamoto, K. R. (1983) *Cell* *35*, 381 – 392.

4. Scheideret, C., Geisse, S., Westphal, H. M. & Beato, M. (1983) *Nature (Lond.) 304*, 749 – 752.

5. Noggle, J. H. & Schirmer, R. E. (1971) *The Nuclear Overhauser Effect – Chemical Applications*, Academic Press, New York.

6. Redfield, A. G. & Gupta, R. K. (1971) *Cold Spring Harbor Symp. Quant. Biol. 36*, 405 – 419.

7. Poulsen, F. M., Hosch, J. C. & Dobson, C. M. (1980) *Biochemistry 19*, 2956 – 2607.

8. Jeener, J., Meier, B. H., Bachmann, P. & Ernst, P. R. (1979) *J. Chem. Phys. 71*, 4546 – 4553.

9. Johnston, P. D. & Redfield, A. G. (1978) *Nucleic Acids Res. 5*, 3913 – 3927.

10. Macura, S. & Ernst, R. R. (1980) *Mol. Phys. 41*, 95 – 117.

11. Kumar, A., Ernst, R. R. & Wüthrich, K. (1980) *Biochem. Biophys. Res. Commun. 95*, 1 – 6.

12. Aue, W. P., Bartholdi, E. & Ernst, R. R. (1976) *J. Chem. Phys. 64*, 2229 – 2246.

13. Bax, A. & Freeman, R. (1981) *J. Magn. Reson. 44*, 542 – 561.

14. Kumar, A., Wagner, G., Ernst, R. R. & Wüthrich, K. (1980) *Biochem. Biophys. Res. Commun. 96*, 1156 – 1163.

15. Wüthrich, K., Wider, G., Wagner, G. & Braun, W. (1982) *J. Mol. Biol. 155*, 311 – 319.

16. Wagner, G., Kumar, A. & Wüthrich, K. (1981) *Eur. J. Biochem. 114*, 375 – 384.

17. Kumar, A., Wagner, G., Ernst, R. R. & Wüthrich, K. (1981) *J. Am. Chem. Soc. 103*, 3654 – 3658.

18. Matteuci, M. D. & Caruthers, M. H. (1981) *J. Am. Chem. Soc. 103*, 3185 – 3191.

19. Seliger, H., Klein, S., Narang, C. K., Seeman-Preising, B., Eiband, J. & Hauel, N. (1982) in *Chemical and Enzymatic Synthesis of Gene Fragments: a Laboratory Manual* (Gassen, G. H. & Lang, A., eds) pp. 81 – 96, Verlag Chemie, Weinheim.

20. Bax, A., Freeman, R. & Morris, G. A. (1981) *J. Magn. Reson. 42*, 164 – 168.

21. Baumann, R., Wider, G., Ernst, R. R. & Wüthrich, K. (1981) *J. Magn. Reson. 44*, 402 – 406.

22. States, D. J., Haberkorn, R. A. & Ruben, D. J. (1982) *J. Magn. Reson. 48*, 286 – 292.

23. Marion, D. & Wüthrich, K. (1983) *Biochem. Biophys. Res. Commun. 113*, 967 – 974.

24. Macura, S., Huang, Y., Suter, D. & Ernst, R. R. (1981) *J. Magn. Reson. 43*, 259 – 281.

25. Clore, G. M. & Gronenborn, A. M. (1984) *FEBS Lett. 172*, 219 – 225.

26. Cheng, D. M. & Sarma, R. H. (1977) *J. Am. Chem. Soc. 99*, 7333 – 7348.

27. Altona, C. (1982) *Recl J. R. Neth. Chem. Soc. 101*, 412 – 433.

28. Wagner, G. & Wüthrich, K. (1979) *J. Magn. Reson. 33*, 675 – 680.

29. Dobson, C. M., Olejniczak, E. T., Poulsen, F. M. & Ratcliffe, R. G. (1982) *J. Magn. Reson. 48*, 97 – 110.

30. Solomon, I. (1955) *Phys. Rev. 90*, 559 – 565.

31. Reid, D. G., Salisbury, S. A., Bellard, S., Shakked, Z. & Williams, D. H. (1983) *Biochemistry 22*, 2019 – 2025.

32. Reid, D. G., Salisbury, S. A., Brown, T., Williams, D. H., Vasseur, J. J., Rayner, B. & Imbach, J. L. (1983) *Eur. J. Biochem. 135*, 307 – 314.

33. Clore, G. M. & Gronenborn, A. M. (1983) *EMBO J. 2*, 2109 – 2115.

34. Clore, G. M. & Gronenborn, A. M. (1984) *Eur. J. Biochem. 141*, 119 – 129.

35. Gronenborn, A. M., Clore, G. M. & Kimber, B. J. (1984) *Biochem. J. 221*, 723 – 736.

36. Clore, G. M., Gronenborn, A. M., Piper, E. A., McLaughlin, L. W., Graeser, E. & van Boom, J. H. (1984) *Biochem. J. 221*, 737 – 751.

37. Scheek, R. M., Russo, N., Boelens, R., Kaptein, R. & van Boom, J. H. (1983) *J. Am. Chem. Soc. 105*, 2914 – 2916.

38. Scheek, R. M., Boelens, R., Russo, N., van Boom, J. H. & Kaptein, R. (1984) *Biochemistry 23*, 1371.

39. Hare, D. R., Wemmer, D. E., Chou, S. H., Drobny, G. & Reid, B. R. (1983) *J. Mol. Biol. 171*, 319 – 336.

40. Weiss, M. A., Patel, D. J., Sauer, R. T. & Karplus, M. (1984) *Proc. Natl Acad. Sci USA 81*, 130 – 134.

41. Feigon, J., Leupin, W., Denny, W. A. & Kearns, D. R. (1983) *Biochemistry 22*, 5943 – 5951.

42. Frechet, D., Cheng, D. M., Kan, L.-S. & Ts'o, P. O. P. (1983) *Biochemistry 22*, 5194 – 5200.

43. Haasnoot, C. A. G., Westerink, N. P., van der Marel, G. A. & van Boom, J. H. (1983) *J. Biomol. Struct. Dyn. 1*, 131 – 149.

44. Roy, S., Redfield, A. G. (1983) *Biochemistry 22*, 1386 – 1390.

45. Hare, D. R. & Reid, B. R. (1982) *Biochemistry 21*, 5129 – 5135.

46. Heerschap, A., Haasnoot, C. A. G. & Hilbers, C. W. (1983) *Nucleic Acids Res. 11*, 4501 – 4520.

47. Gronenborn, A. M., Clore, G. M., Jones, M. B. & Jiricny, J. (1984) *FEBS Lett. 265*, 216 – 222.

48. Patel, D. J., Kozlowski, S. A., Marky, L. A., Broka, C., Rice, J. A., Irakura, K. & Breslauer, K. J. (1982) *Biochemistry 21*, 428 – 436.

49. Dickerson, R. E. & Drew, H. R. (1981) *J. Mol. Biol. 149*, 761 – 786.

50. Arnott, S. & Hukins, D. W. L. (1972) *Biochem. Biophys. Res. Commun. 47*, 1504 – 1509.

51. Dickerson, R. E., Drew, H. R., Conner, B. N., Wing, R. M., Fratini, A. V. & Kopka, M. L. (1982) *Science (Wash. DC) 216*, 475 – 485.

52. Shakked, Z., Rabinovich, D., Kennard, D., Cruse, W. B. T., Salisbury, S. A. & Viswamitra, A. (1983) *J. Mol. Biol. 166*, 183 – 201.

53. Conner, B. N., Yoon, C., Dickerson, J. L. & Dickerson, R. E. (1984) *J. Mol. Biol. 174*, 663 – 695.

54. Clore, G. M. & Gronenborn, A. M. (1985) *J. Magn. Reson.*, in the press.

55. Feigon, J., Wright, J. M., Leupin, W., Denny, W. A. & Kearns, D. R. (1982) *J. Am. Chem. Soc. 104*, 5540 – 5541.

G. M. Clore, H. Lauble, and A. M. Gronenborn, Max-Planck-Institut für Biochemie, Am Klopferspitz 18a, D-8033 Martinsried, Federal Republic of Germany

T. A. Frenkiel, Medical Research Centre Biomedical Nuclear Magnetic Resonance Centre, National Institute for Medical Research, Mill Hill, London, England NW7 1AA